BRILL

Timing & Time Perception (*2015*) DOI:10.1163/22134468-03002042

TIME

brill.com/time

Imagined Temporal Groupings Tune Oscillatory Neural Activity for Processing Rhythmic Sounds

Brandon T. Paul[1,*], **Per B. Sederberg**[2] **and Lawrence L. Feth**[1]

[1] Department of Speech and Hearing Science, The Ohio State University, Columbus, OH 43210, USA

[2] Department of Psychology, The Ohio State University, Columbus, OH 43210, USA

Received 17 April 2014; accepted 3 December 2014

Abstract

Temporal patterns within complex sound signals, such as music, are not merely processed after they are heard. We also focus attention to upcoming points in time to aid perception, contingent upon regularities we perceive in the sounds' inherent rhythms. Such organized predictions are endogenously maintained as *meter* — the patterning of sounds into hierarchical timing levels that manifest as *strong* and *weak* events. Models of neural oscillations provide potential means for how meter could arise in the brain, but little evidence of dynamic neural activity has been offered. To this end, we conducted a study instructing participants to imagine two-based or three-based metric patterns over identical, equally-spaced sounds while we recorded the electroencephalogram (EEG). In the three-based metric pattern, multivariate analysis of the EEG showed contrasting patterns of neural oscillations between strong and weak events in the delta (2–4 Hz) and alpha (9–14 Hz), frequency bands, while theta (4–9 Hz) and beta (16–24 Hz) bands contrasted two hierarchically weaker events. In two-based metric patterns, neural activity did not drastically differ between strong and weak events. We suggest the findings reflect patterns of neural activation and suppression responsible for shaping perception through time.

Keywords

EEG, neural oscillations, meter, rhythm, partial least squares analysis, timing

1. Introduction

An unresolved problem in human sensory perception is how the brain tracks rhythmic sound structures, such as speech and music, through time. Regularity

* To whom correspondence should be addressed. E-mail: paulbt@mcmaster.ca. Present address: Department of Psychology, Neuroscience, & Behaviour, McMaster University, Hamilton, ON L8S 4K1, Canada

DOI: 10.1163/22134468-03002042

in the temporal patterning of these sounds helps listeners build predictions and coordinate action to prepare for *what* is likely to occur and *when* (reviewed extensively in Repp, 2005; Repp & Su, 2013). Dynamic attending theory (DAT) has been invoked to account for these phenomena, positing that attentional focus and thus perception is highest at time points that are most predicted (Jones, 1976; Jones & Boltz, 1989). An important facet of this experience is that it unfolds in a hierarchy, referred to as *meter*. For example, musical beats (the periodic percepts to which a listener might tap a foot or nod their head) are metrically structured as harmonically-related periodic levels relating in integer ratios such as 1:2 and 1:3 (Lerdahl & Jackendoff, 1983). Higher-level metric structure is experienced as a periodicity of *strong* beats that start the group, each of which is followed by one or more *weak* beats of lower-level. In the view of DAT, attention should be highest at strong beats and lower at weak beats (Large & Jones, 1999). Indeed, listeners can volitionally impose a metric hierarchy on ambiguous rhythms that can influence memory and perception for rhythmic sounds (Palmer & Krumhansl, 1990).

Though meter is inherent to rhythmic behavior and facilitates perception, it is less clear how it is maintained in the brain. Neural entrainment models propose that perceived rhythmic structures drive endogenous harmonically-related neural oscillations that hierarchically direct attention to predicted time points (Large, 2008; Large & Jones, 1999; Large & Snyder, 2009; van Noorden & Moelants, 1999), suggesting that metric representations are observable by recording oscillatory neural activity from the scalp. Specifically, peaks of attention in DAT are theorized to arise as slow oscillations locked to the rate of the beat and higher metric levels (Henry & Hermann, 2014). In support, Nozaradan et al. (2011, 2012) reported steady-state evoked brain responses at subharmonic frequencies (i.e., longer beat periods not accounted for by physical stimulus energy) corresponding to listeners' intended metric interpretations. However, these results do not speak to the dynamic time course of neural changes between each metric beat that explain the behavior of neural populations in support of meter. Imagined strong and weak beats are associated with different event-related potentials (Schaefer et al., 2011) and magnetic fields (Fujioka et al., 2010). Brain responses to rhythmic violations also vary between strong and weak beats, suggesting separate sensory or predictive processes depend on metric stress (Brochard et al., 2003; Snyder & Large, 2005).

However, little is known about the behavior of oscillatory neural activity when rhythms are imagined with different types of meter. Using an ambiguous rhythm of two beats and a rest (silence), Iversen et al. (2009) found that evoked beta (20–30 Hz) power is higher on the beat chosen to be strong, but only focused on interpretations of the same metric type and did not contrast different metric types. Thus, the primary goal of the present study was to identify previously-unknown patterns of oscillatory neural activity recorded from the scalp that relate to strong and weak metric positions in two different types of meter while also analyzing all frequency bands. A second goal was to examine if stimulus deviance

detection was improved on strong beats versus weak beats as listeners imagined meter, predicted by DAT. Findings overall are discussed in terms of excitatory (Arnal & Giraud, 2012; Henry & Hermann, 2014) and inhibitory (Weisz et al., 2011) activity related to maintaining a metric representation.

2. Materials and Methods

2.1. Participants

Sixteen right-handed participants with self-reported normal hearing (7 females; mean age = 24.6 years; range = 19–31 years) volunteered for the study and provided written consent after being informed of the study's procedures. They were compensated 20 USD for participation. The study's procedures were consistent with the Declaration of Helsinki and were approved by the Institutional Review Board at The Ohio State University.

2.2. Stimuli and Materials

The experimental task was to imagine meter over a series of rhythmic stimuli while also detecting the presence of a deviant stimulus. Each stimulus comprising the sequence was constructed of a pair of 0.25 ms wideband sound pulses (Ronken, 1970) generated in Python (Fig. 1). Pulses differed in amplitude by one half; one pulse was delivered at 106 dB peak-equivalent sound pressure level (peSPL) and the other at 100 dB peSPL. It should be noted that peSPL is the sound pressure level in dB of a 1000 Hz tone with peak amplitude equal to the amplitude of the transient pulse. This is a standard way to reference the intensity level of a transient signal, but it is not related to the energy or power in the transient. Click pairs could be presented such that the higher intensity pulse occurred before or after the lower intensity pulse, thus yielding frontwards and backwards stimulus types. In this sense, the power spectrum was equated for both stimulus types, and the frontwards and backwards stimuli only differ in their phase spectrum (for additional information on the properties of these click pairs, see Ronken, 1970). The timing distance between each click pulse determines the discriminability in phase between frontward and backwards presentations. To equate discriminability performance across subjects, each participant performed a two-alternative forced choice task

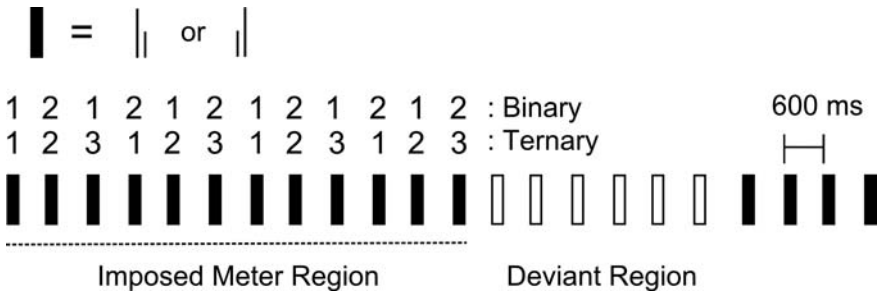

Figure 1. Stimulus sequences used in the task. Each black bar represents frontward- or backward-presented click pairs. Participants counted along with the pattern according to metric type during the entire sequence. Deviant click pairs arise only once per trial in a random position of the deviant region. Priming sequences are not shown.

within a one-up three-down adaptive procedure across three trial blocks to determine the timing between the pulses so that stimuli were discriminable with 79% accuracy (Levitt, 1971). This procedure was completed before the main experiment. Timing separation values across subjects ranged between 10.4 and 11.9 ms (M = 11.5 ms). These sound pulse pairs were used as individual stimuli in the rhythmic task.

The rhythmic task is shown in Fig. 1 and is adopted from a procedure similar to Potter et al. (2009). Trial sequences consisted of 22 click pairs with a 600 ms inter-onset interval (IOI). Between the 13th and 18th position in the sequence, a reversed-order click pair was presented as a deviant stimulus. For example, if the trial sequence consisted of frontward click pairs, the deviant stimulus is one backward click pair. The position of the deviant was randomly chosen for each trial. The choice of stimulus context, being non-deviant frontward or backward click pairs, was randomized across all trials. Participants were unaware of the stimulus context presented during each trial, and unaware that target stimuli were confined to specific positions. Stimuli were presented binaurally through Etymotic Research 3A insert phones connected to an Apple MacBook Pro with a 2.66 GHz Intel Core i7 processor. Audio was controlled using the RtAudio library (Scavone, 2001) built into the Python Experiment-Programming Library (PyEPL; Geller et al., 2007). Participants responded behaviorally through a wireless (Bluetooth) keyboard to an experimental interface also built using the PyEPL.

2.3. Procedure

We instructed participants to count sound onsets in groups of two (binary meter) and groups of three (ternary meter). Participants mentally counted "one, two, three; one, two, three…" in ternary conditions and "one, two; one, two…" in binary conditions as sounds were presented (Fig. 1). Participants were instructed not to move in time with the stimuli nor vocalize the mental counting. To start each trial, participants were primed with a sequence of 100 ms sine tones presented at 600 ms IOI that outlined the binary and ternary meters: 720 Hz sine tones signified strong beats and 440 Hz sine tones signified weak beats. Following the primes, 1000 ms of silent space jittered by +/– 400 ms elapsed before click sequences began. This priming sequence reminded subjects of the appropriate meter to use, but prevented a direct continuation of cued meter that might bias organization of the test stimuli with imagined frequency differences. While imposing meter over the subsequent click sequence, participants listened for the deviant. After each sequence completed, participants reported the metric position on which a deviant stimulus occurred using keyboard keys *1, 2,* or *3; 1* and *2* were used for binary meter and all three numbers were used for ternary meter. Sessions consisted of five binary and five ternary blocks that were shuffled randomly. Each trial block contained 12 sequences of randomly-shuffled stimulus contexts of frontward- and backward-presented clicks. Before each block began, computer screen text informed participants of what metric organization to use.

2.4. Electrophysiological Recording and Preprocessing

The electroencephalogram (EEG) was recorded in an electrically-shielded and sound-attenuated room via a 128-electrode Brain Products actiCAP system (BrainProducts GmbH, Munich, Germany) utilizing a 96-electrode montage connected to a Brain Products actiCHamp amplifier. The electrooculogram (EOG) was also recorded by a channel under the left eye. EEG signals were recorded by a Dell Optiplex 980 desktop computer with a 2.5 GHz Intel Core i5 vPro processor sampling data at 1000 Hz. Using the Python Time Series Analysis (PTSA) library (http://ptsa.sourceforge.net), data were first re-referenced offline to linked mastoids and high-pass filtered above .25 Hz. A wavelet-enhanced independent components analysis algorithm corrected for eyeblink and motion artifacts without having to reject events due to movement or muscle interference (Castellanos & Makarov, 2006). The algorithm identifies eyeblink and motion artifacts using

data recorded from the EOG, and then corrects these high-power low-frequency signals while preserving higher frequency EEG data. Epochs of data were set between -250 to 1000 ms with 0 ms corresponding to event (beat) onset, downsampled to 200 Hz, and their spectral power was calculated through Morlet wavelets (five wave cycles) using frequency bins of delta (2–4 Hz), theta (4–8 Hz), alpha (9–14 Hz), beta (16–26 Hz), low gamma (28–42 Hz), and high gamma (44–100 Hz). For each wavelet a Gaussian window was applied, meaning in the cases of delta activity where power calculations are less accurate over the 1 s epoch, oscillatory power is reasonably estimated at the peak. Data were then averaged around each metric condition of binary strong beat (B1, $N = 360$ per subject), binary weak beat (B2, $N = 360$), ternary strong beat (T1, N = 240), first ternary weak beat (T2, $N = 240$), and second ternary weak beat (T3, $N = 240$). Resulting total power values for each time point, channel, and frequency were converted to z-transformed log power and further downsampled to 50 Hz. Final data for statistical analysis were either baseline corrected from -100 to 0 ms prior to each event onset (to examine event-related changes in total oscillatory power) or left uncorrected at the baseline to examine global states of oscillatory power. Data uncorrected at the baseline may measure neural activity not strictly time-locked to each beat but rather oscillatory activity related to the metric type (e.g., binary vs. ternary).

2.5. Statistical Analysis

To examine brain activity during conditions when sounds did not change, the analysis focused only on brain responses during the first 12 onsets (the imagined meter region) of the trial sequence. The priming sequence and deviant region were not subject to neural response analysis. We used mean-centered task partial least-squares (PLS) analysis (Krishnan et al., 2011; McIntosh & Lobaugh, 2004) implemented in MATLAB (The MathWorks, Natick, MA) to identify maximally-orthogonal patterns of neural activity across the experimental conditions (used similarly by Fujioka et al., 2010, on event-related magnetic fields but not oscillatory activity). The PLS algorithm correlated a matrix of neural data (z-transformed log power values for all electrodes, time points, and frequencies for each subject) to a matrix of design data (pre-defined metric conditions of B1, B2, T1, T2, and T3) using a least-squares optimization to yield linear combinations of these elements referred to as latent variables (LVs). LVs can be positive or negative and consist of *saliences* that indicate the strength of relationship between data in the neural matrix to the matrix of metric positions (design matrix). Statistical significance was assessed by a permutation test that runs the PLS algorithm on the spatiotemporal matrix of brain saliences over 500 iterations. LVs occurring in more than 95% of total iterations were retained and deemed to be significant. To identify the stable features supporting significant LVs, a 100-sample bootstrap test (with replacement) identified electrodes within each frequency band and time point (each of which expressed by a salience value) whose bootstrap ratios fall above the 0.975 threshold. Using this approach, significance was assessed within the permutation tests whereas bootstrap tests describe the reliability. Thus, no multiple comparisons corrections were needed when salience values of time points, channels, and electrodes were compared in bootstrap tests (McIntosh & Lobaugh, 2004). For further information on resampling techniques such as bootstrap and permutation tests, see Rodgers (1999).

3. Results

3.1. Behavioral Results

Behavioral performance on the deviant identification task was analyzed as the proportion of correct trials (pc). Chance levels were 0.5 for binary metric conditions and 0.33 for ternary metric conditions. Participants performed above chance for both binary metric conditions (B1 pc = 0.57; B2 pc = 0.58) and for T1 (pc = 0.46)

and T2 (pc = 0.47) but not T3 (pc = 0.31). Behavioral responses were examined using a binomial logistic regression in the R statistics package. Results from the logistic regression indicate that ternary meter overall led to incorrect responses more frequently than binary meter ($\chi^2 = 21.067$, $p < 0.001$; odds ratio (OR) = 1.61). Between beats, T3 led to incorrect responses more than T1 ($\chi^2 = 19.05$, $p < 0.001$; OR = 1.54) but no response difference was found between T1 and T2 ($p = 0.524$; OR = 1.11) or between B1 and B2 ($p = 0.526$; OR = 1.08). Surprisingly, detecting frontwards clicks in a context of backwards clicks led to incorrect responses more than the opposite ($\chi^2 = 7.46$, OR = .78, $p = 0.006$), but examining each click-pair context separately did not change results in relation to effects of metric position or metric type. All further analysis herein combines contexts of frontward and backward click pairs together.

3.2. Electrophysiological Results

3.2.1. Baseline Corrected Data

The PLS algorithm identified two significant LVs. The first LV (LV1, $p < 0.001$; accounting for 47.0% of cross-block covariance) contrasted oscillatory brain activity for T1 versus all other metric positions (aside from B2) but most strongly against T2 and T3 (Fig. 2a). To identify the elements that contribute to this arrangement of contrasts, we plotted topographic maps that reflect each electrode's salience in the LV for each frequency band and all time points separated by 20 ms intervals (Fig. 3a). Examining each plot visually, we identified representative electrodes whose power reliably contributed to the LV as determined by bootstrap tests and depicted by emboldened dots on topographic maps. Time points within time series plots of spectral power reliably contributing to the LV are noted by hexagonal stars above each set of traces. As shown in Fig. 3a, alpha power increased after T1 from 400 ms into T2 onset at 600 ms, dropping only

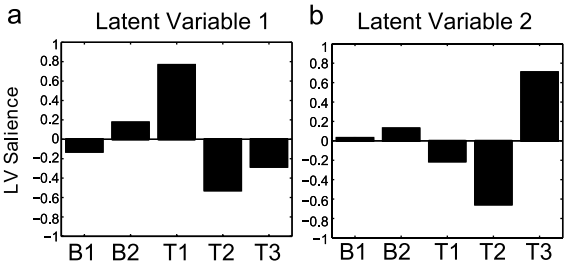

Figure 2. Salience plots of latent variables (LVs). Salience values indicate how strongly frequencies, time points, and channels of spectral power explain pre-defined conditions of metric beats. **(**a) LV1 contrasts T1 against T2 and T3 and corresponds to topographies and time series in Fig. 3. (b) LV2 contrasts T3 against T1 and T2 and corresponds to topographies and time series plots in Fig. 4.

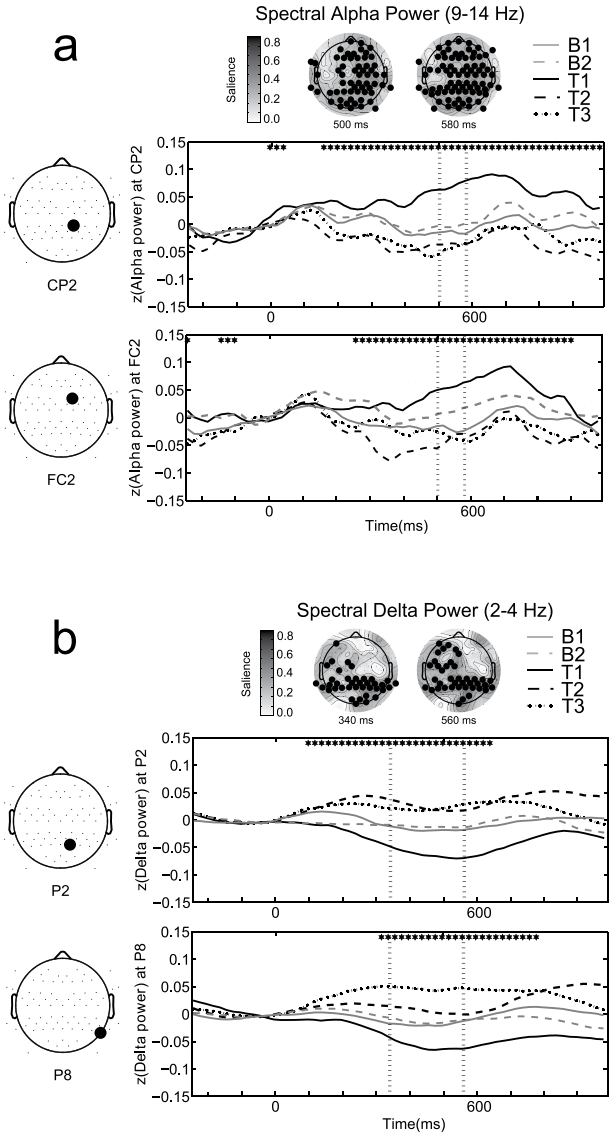

Figure 3. Topographies and time series of normalized spectral alpha and delta power corresponding to LV1. Topographic maps are shown with shading corresponding to each channel's salience to LV1 in the alpha band; channels that reliably contribute to LV1 determined by bootstrap tests are indicated by emboldened dots. Two representative electrodes' normalized spectral power is plotted as time series waveforms. Vertical dashed lines in time series correspond to time points at which topographies are plotted, and asterisks denote time points reliably contributing to LV1. The 0 ms mark on time series plot abscissa indicates onset of a stimulus and the 600 ms indicates the onset of the subsequent stimulus. (a) Topographies and time series for alpha power. (b) Topographies and time series for delta power.

after 700 ms (100 ms after T2). This pattern of activity is reflected in the majority of the channel array but most strongly in right central channels. The time course of alpha power was similar after each metric beat, but alpha power after T2 and T3 did not increase as strongly as did power for T1, consistent with the contrasts made by the PLS algorithm (Fig. 2a). B1 and B2 showed very similar time courses during alpha activity, and qualitatively oppose the pattern show for ternary conditions with alpha power being highest before B1. Figure 3b depicts an opposing pattern for delta power across parietal channels, which decreased after T1 at 300 ms into T2 and recovering after T2 onset. Delta power did not drop as severely for other metric positions and is most shallow following T2 and T3, matching the temporal pattern exhibited in the delta band. Delta power after B1 and B2 however are qualitatively similar.

LV2 (p = 0.034) accounted for 24.0% of the cross-block covariance (Fig. 2b). In this LV, oscillatory power during T3 contrasted strongly to T2 and less so to T1. Spatiotemporal brain patterns are subsequently investigated considering this contrast. As shown in Fig. 4a, peaks in beta power arose in the T3 trace before T1 from 440 to 560 ms in centrally distributed and parietal electrodes. Beta power in these channels after T2, however, dipped during this time period, and increased in power just after T3 from 30 to 110 ms. T1 beta power does not appear to modulate around beat events as does T2 and T3. B1 and B2 do not show differentiable patterns. A complimentary relationship in theta power is depicted in Fig. 4a in right temporal channels, which dropped strongly before T1 onset (following the T3 trace) and weakly before T2 and T3 (following the T1 and T2 traces, respectively).

3.2.2. Data Uncorrected at the Baseline

We ran the PLS algorithm on data not corrected at the baseline to compare condition-related (not event-related) global states of oscillatory power. The algorithm identified one significant LV (LV3, p = 0.012, accounting for 74.0% of the cross-block covariance) contrasting binary and ternary conditions, but not between metric beats (Fig. 5a). Examining topographies and power time series from follow-up bootstrap tests, increased high spectral gamma power (44–100 Hz) persisted across posterior channels during B1 and B2 conditions when compared to T1, T2, and T3 (Fig. 5b).

4. Discussion

4.1. Summary

We conducted a study requiring participants to imagine binary and ternary metric groupings over isochronous sequences with identical sounds while detecting the presence of a deviant stimulus. Since previous research addresses the time course of averaged event-related potentials correlating to these metric groupings

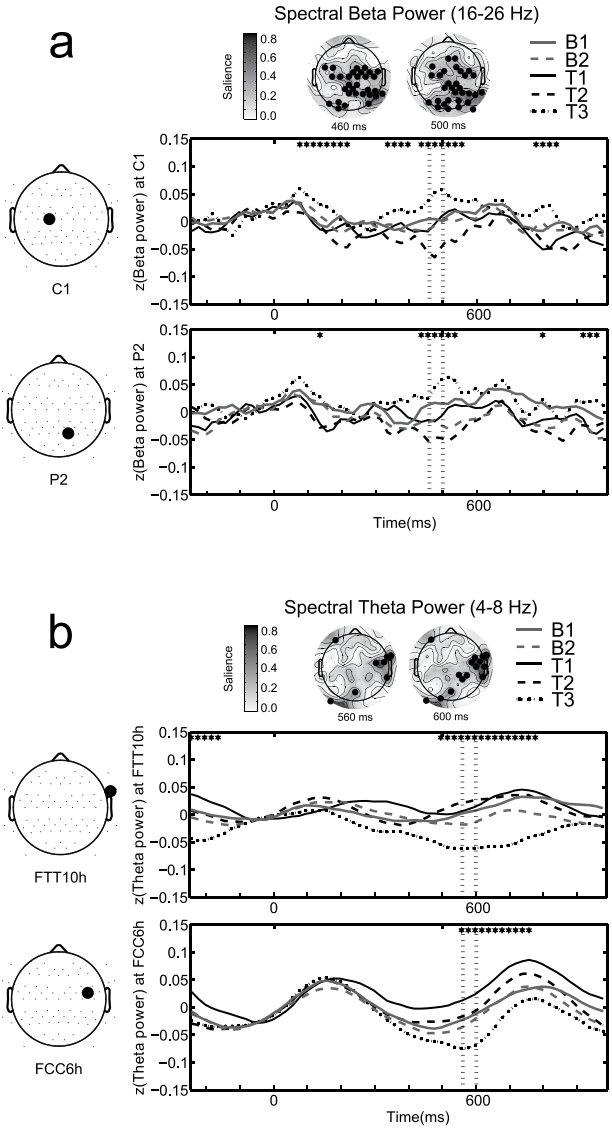

Figure 4. Topographies and time series of spectral power for components corresponding to LV2. (a) Topographies and time series for beta power. (b) Topographies and time series for theta power. See caption of Fig. 3 for details of topographic plots and time series plots.

(Fujioka et al., 2010; Schaefer et al., 2011), we focused here on oscillatory correlates of imagined meter using a multivariate approach. A first arrangement of contrasts showed that alpha power distributed broadly across the electrode array increased most strongly before T2 onset whereas alpha power before T1 and T3 were less strong. Meanwhile, delta power in parietal channels decreased most

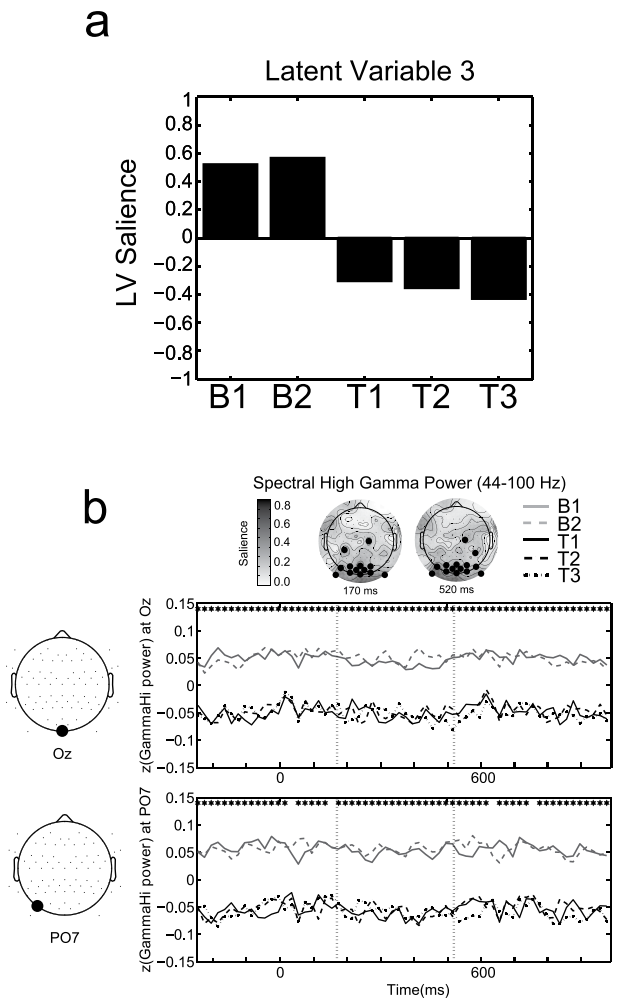

Figure 5. (a) Salience plot for data uncorrected at the baseline. (b) Topographies of channels reliably contributing to LV3 in the high gamma band and two representative electrodes' power time series.

strongly before T2 and less so for T1 and T3. A second arrangement of contrasts showed that beta power in central channels increased before T1 and decreased before T3. Theta power in right temporal channels decreased most strongly before T1 and only weakly before T2 and T3. Strong contrasts in binary meter were not identified. These novel results suggest fast and slow neural oscillations can be tuned by imagined ternary meter and may represent fluctuating levels of neural excitability underpinning a metric representation. Behaviorally, binary meter overall led to better detection of deviant stimuli. B1 and B2 metric positions did not lead to significant differences in performance. In ternary meter, deviant detection was worst on T3, and detection did not differ between T1 and T2.

4.2. Behavioral Performance Relating to Dynamic Attending Theory

Dynamic attending theory (DAT) predicts greater attention and improved perception for strong beats compared to weak beats in metric sequences (Jones & Boltz, 1989). In agreement, strong beats in metric contexts are linked to faster reaction times to deviant sounds (Bolger et al., 2014), improved detection of stimulus change (Grube & Griffiths, 2009), and improved semantic processing in language (Rothermich et al., 2012). Behavioral results in the present study are not entirely consistent with this notion. A significant performance decrement was found on T3 where attention is predicted to be weakly focused, consistent with DAT. However no significant differences were found between T1 and T2 or B1 and B2, and contrary to DAT, performance on T2 and B2 was qualitatively higher than strong beats T1 and B1 respectively. The task difficulty of the current experiment may explain these inconsistencies. At the outset, the pre-experiment psychophysical task aimed to equate performance across participants such that stimuli could be differentiated at 79% accuracy in an alternative forced choice task. Despite this, the performance on the rhythmic task was marginally above chance and well below 79%. One possible explanation is that the rhythmic detection task significantly lowers accuracy as a result of more alternative choices, obscuring results interpretable under DAT. Another possibility is that attentional pulses predicted by DAT are not robust to discriminate the temporal order of brief sounds. A further complication is that participants performed better when required to identify backwards clicks in a context of frontwards clicks, which is not consistent with previous findings that frontward clicks and backwards clicks are equally discriminable (Ronken, 1970). The rhythmic task here may have uncovered a perceptual asymmetry in listeners' ability to resolve the phase spectra of brief stimuli.

4.3. Separate Oscillatory Responses to Metric Beats Related to Excitation and Inhibition

Neural oscillations in frequency ranges greater than 10 Hz are linked to an array of attention and timing processes (Arnal, 2012; Ward, 2003). For example, alpha power observed during attention tasks is linked to top-down activation of inhibitory circuits across the cortex (Klimesch et al., 2007), where greater alpha synchronization reflects cortical suppression in both auditory (Weisz et al., 2011) and visual (Jensen et al., 2012) tasks. Top-down expectation appears to modulate alpha power, which is shown to desynchronize before an anticipated sound (Hartmann et al., 2012) and synchronize before predictable ignored sounds (Gomez-Ramirez et al., 2011). Alpha power in the present study increased before T2 broadly across central electrodes, which may likewise reflect the engagement of inhibitory circuits functioning to suppress the neural representation of T2. In contrast, beta power peaked before T1 across central channels whereas beta power decreased prior to T3. Recent studies report beta activity to synchronize before expected sounds as anticipated beats unfolded in an isochronous sequence. When the rhythmic

regularity is high, observed anticipatory synchronous beta activity is stronger, suggesting that beta power in this context underpins the brain's representation of beat timing (Fujioka et al., 2009, 2012) Listeners can also choose which beat of a two note rhythm should have metric stress, which correlate with an increase in beta power (Iversen et al., 2009). The present data are consistent with these findings and can be interpreted similarly: Predictions are greater for chosen strong beats and are reflected as higher beta power before T1; conversely, predictions are less strong for T3, leading to anticipatory decreases in beta power. Together, we suggest pre-stimulus beta activity might reflect greater attention directed at strong beats and that alpha activity gates attentional focus so that it is weaker.

Slow-wave oscillations are implicated in auditory and visual predictive timing (Gomez-Ramirez et al., 2011; Lakatos et al., 2008; see Arnal & Giraud, 2012; Giraud & Poeppel, 2012, for reviews) and may play a fundamental role in tracking and predicting the stimulus periodicity (Schroeder & Lakatos, 2009). A recent review by Henry and Hermann (2014) theorized that delta and theta activity directly reflect attentional focus directed at predicted time points hypothesized by DAT (Jones, 1976; Large & Jones, 1999). Results here support the notion that these frequency bands are implicated in hierarchically-structured timing. As alpha power increased before T2, delta power dropped during the same time period. As beta power peaked before T1, theta power dropped as T1 occurred. Although the spatial relationships between alpha/delta and beta/theta do not overlap, the temporal profiles may suggest slower-wave oscillations organize faster alpha and beta oscillations across distributed cortical networks, in sum underpinning the metric representation (Arnal & Giraud, 2012). Arnal et al. (2014) reported that the strength of coupling between delta oscillation phase and beta power predicts the accuracy of detecting a temporally-displaced deviant target in a short isochronous sequence of notes. Although Arnal et al. (2014) did not manipulate imagined metric structure, results here suggest that coupling between theta or delta and beta oscillations will be greater before strong beats. The opposite may hold for weak beats, wherein slow-wave oscillations couple with alpha activity during stimulus suppression of weak beats. Near-field electrophysiological recordings over auditory cortex during an attending task performed by Gomez-Ramirez et al. (2011) accordingly show that delta phase couples with alpha power strongly before sounds that are to be ignored. In sum, modulation of linked fast and slow oscillations may be a neural correlate of predictive timing and attention (Calderone et al., 2014). The present results show for the first time that these patterns may be tuned by a volitionally-imposed metric structure, suggesting increased neuronal excitability (theta–beta) before strong beats and increased neuronal inhibition (delta–alpha) before weak beats.

4.4. Neural Activity and Behavioral Performance Did not Differ in Binary Metric Positions

Although the PLS algorithm identified neural contrasts in ternary meter, results for binary meter were inconclusive. One interpretation of this finding is that cognitive

resources during binary meter were more strongly allocated to the detection task, since it is reasonable to argue that counting in groups of two is simpler than counting in threes. A more complex meter (e.g., ternary) would require greater cognitive resources, generating a stronger representation that is indeed seen in the present data. A less complex meter (e.g., binary) would free cognitive resources that are able to be reallocated to the detection task. Further support is offered by the observation that binary meter is more common in Western music than ternary meter (Huron, 2006) and exposure to meter throughout development shapes metric preferences (Soley & Hannon, 2010). Western-enculturated listeners recruited for the present study might then require less cognitive resources to maintain a binary structure. Behavioral results support this notion, as participants were 1.6 times more likely to identify a deviant stimulus correctly in binary meter versus ternary meter.

This interpretation is consistent with LV3 on data not corrected at the baseline that compared global states of oscillatory power that persist across trials. The analysis revealed increased high gamma power across posterior channels during all binary metric beats compared to all ternary beats (Fig. 5). Previous research suggests that gamma power is sensitive to attentional states and may reflect synchronization of neural populations implicated in selective attention in both visual and auditory modalities (e.g., Doesburg et al., 2012; Fries et al., 2001; Gregoriou et al., 2009; Schroeder & Lakatos, 2009). Although the strongly occipital topography of high gamma activity is unusual in auditory tasks and is typically seen in visual tasks, sustained auditory attention (such as that required in the present detection task) engages the visual cortex and, here, may be the correlate of increased high-gamma activity during binary conditions (Cate et al., 2009). A shortcoming to this interpretation is that low-frequency neural oscillations are predicted to decrease at the cost of increasing the power in high-frequency (gamma) oscillations during a vigilance-style auditory task (Schroeder & Lakatos, 2009) and in the present data no differences in power were found in any band below 44 Hz.

There are several alternative considerations that may explain inconclusive results in binary meter and its correlation to high-gamma power. It is possible that high-gamma activity in occipital channels reflects electromyographic activity of head and neck muscles that may be greater during binary metric attending, however this activity typically peaks under 20 Hz (Tissen et al., 2000) but does have power extending to 100 Hz (Van Boxtel et al., 2001). High gamma activity might also reflect microsaccadic activity in occipital channels, however oscillations resulting from microsaccades most strongly manifest when using a nose reference during EEG recording (Melloni et al., 2009) whereas the current study used a linked-mastoid reference. Another alternative explanation is that binary meter unfolds over a shorter overall period than ternary meter and thus does not produce as strong a signal regardless of cognitive effort, and a quaternary condition might better serve as a contrast in this design. Despite these limitations, we suggest binary meter may not require an abundance of attentional resources due to ease and/or enculturation, and its dynamics are consequently obscured by the

noise of the EEG. Ternary meter requires resources to maintain, in turn providing a stronger EEG signal. Taken together, a lack of contrast in binary-based meter does not discount oscillatory activity patterns identified for ternary meter.

4.5. Limitations

The present study has noteworthy limitations. First, including trials in the analysis that yielded both incorrect and correct responses introduces the possibility that a metric representation was not properly maintained during each trial, adding excessive noise to the dataset due to the absence of a manipulation check separate from the detection task. Second, participants mentally counted sound onsets in order to determine the metric position of deviant stimuli. Although we informed participants to not vocalize counting, there is a possibility that participants subvocalized, leading to the activation of vocal muscles. Since an electrophysiological measure to identify vocal activations was not used, we cannot rule out the possibility that the artifact correction algorithm did not remove these activations. Similarly, mental counting may have created a linguistic representation of numbers themselves that are reflected in the data, unrelated to the metric representation. However in this case, likewise numbers in both conditions ('ones' and 'twos', for example) are expected to create similar patterns of neural activity regardless of metric condition. Observable relationships between B1 and T1 and B2 and T2 were not qualitatively present in the data. Finally, as discussed, participant performance during the rhythmic task fell far below the target accuracy of 79 to 57.5% for binary and 41.3% for ternary. We believe that the increased number of forced-choice options in the rhythmic task (at most 22 comparisons) produced lower accuracy values than indicated in the pre-experiment task (two alternative forced choice) and limits the conclusions able to be drawn against dynamic attending theory.

4.6. Conclusions and Hypotheses for Future Research

Using an exploratory multivariate technique, we identified the time course of fast- (alpha, beta) and slow- (delta, theta) wave oscillations related to the volitional metric organization of isochronous, identical sounds, in line with neural activity predicted by entrainment models of metric attending (Large, 2008; Large & Jones, 1999; van Noorden & Moelants, 1999) . Based on these new results and their interpretation, we make four key hypotheses for neural oscillations in metric attending: 1) Pre-stimulus alpha activity reflects anticipatory inhibition, increases prior to metric events that are weaker in a metric hierarchy, and functions to narrow sensory gating to diminish perception; 2) Pre-stimulus beta activity reflects anticipatory facilitation, increases prior to strong metric events, and broadens sensory gating to improve perception; 3) Delta and theta activity are modulated by the metric period and functionally organize inhibitory and excitatory circuits reflected in alpha and beta frequency bands, respectively (also predicted by Henry

& Hermann, 2014); 4) Binary metric organization requires less neural resources than ternary or more complex metric organization in a population of Western-music listeners, and gamma activity can index the level to which meter-related neural resources are engaged. Listeners with a musical culture exhibiting predominantly ternary-based metric structures will show the opposite. We invite future research to test these claims.

Acknowledgements

This work was supported in part by a grant from the Office of Naval Research (#N000140911017) to L.L.F. We thank two anonymous reviewers for their comments.

Conflict of interest

The authors declare no competing financial interests.

References

Arnal, L. J. (2012). Predicting "when" using the motor system's beta-band oscillations. *Front. Hum. Neurosci, 6*, 225. doi:10.3389/fnhum.2012.00225.

Arnal, L. H., & Giraud, A. L. (2012). Cortical oscillations and sensory predictions. *Trends Cogn. Sci., 16*, 390–398.

Arnal, L. H., Doelling K. B., & Poeppel, D. (2014). Delta–beta coupled oscillations underlie temporal prediction accuracy. *Cereb. Cortex*, bhu103. doi:10.1093/cercor/bhu103.

Bolger, D., Coull, J. T., & Schön, D. (2014). Metrical rhythm implicitly orients attention in time as indexed by improved target detection and left inferior parietal activation. *J. Cogn. Neurosci.*, *26*, 593–605.

Brochard, R., Abecasis, D., Potter, D., Ragot, R., & Drake, C. (2003). The "ticktock" of our internal clock: Direct brain evidence of subjective accents in isochronous sequences. *Psychol. Sci.*,*14*, 362–366.

Calderone, D. J., Lakatos, P., Butler, P. D., & Castellanos, F. X. (2014). Entrainment of neural oscillations as a modifiable substrate of attention. *Trends Cogn. Sci., 18*, 300–309.

Castellanos, N. P., & Makarov, V. A. (2006). Recovering EEG brain signals: Artifact suppression with wavelet-enhanced independent component analysis. *J. Neurosci. Meth., 158*, 300–312.

Cate, A. D., Herron, T. J., Yund, E. W., Stecker, G. C., Rinne, T., Kang, X., Petkov, C. I., Disbrow, E. A., & Woods, D. L. (2009). Auditory attention activates peripheral visual cortex. *PLoS One, 4*, e4645. doi: 10.1371/journal.pone.0004645.

Doesburg, S. M., Green, J. J., McDonald, J. J., & Ward, L. M. (2012). Theta modulation of inter-regional gamma synchronization during auditory attention control. *Brain Res., 1431*, 77–85.

Fries, P., Reynolds, J. H., Rorie, A. E., & Desimone, R. (2001). Modulation of oscillatory neuronal synchronization by selective visual attention. *Science, 291*, 1560–1563.

Fujioka, T., Trainor, L. J., Large, E. W., & Ross, B. (2009). Beta and gamma rhythms in human auditory cortex during musical beat processing. *Ann. N.Y. Acad. Sci.*, *1169*, 89–92.

Fujioka, T., Zendel, B. R., & Ross, B. (2010). Endogenous neuromagnetic activity for mental hierarchy of timing. *J. Neurosci., 30*, 3458–3466.

Fujioka, T., Trainor, L. J., Large, E. W., & Ross, B. (2012). Internalized timing of isochronous sounds is represented in neuromagnetic beta oscillations. *J. Neurosci., 32*, 1791–1902.

Geller, A. S., Schleifer, I. K., Sederberg, P. B., Jacobs, J., & Kahana, M. J. (2007). PyEPL: A cross-platform experiment-programming library. *Behav. Res. Meth., 39*, 950–958.

Giraud, A. L., & Poeppel, D. (2012). Cortical oscillations and speech processing: Emerging computational principles. *Neurosci. Nat. Neurosci.*, *15*, 511–517.

Gomez-Ramirez, M., Kelly, S. P., Molholm, S., Sehatpour, P., Schwartz, T. H., & Foxe, J. J. (2011). Oscillatory sensory selection mechanisms during intersensory attention to rhythmic auditory and visual inputs: A human electro-corticographic investigation. *J. Neurosci., 31*, 18556–18567.

Gregoriou, G. C., Gotts, S. J., Zhou, H., & Desimone, R. (2009). High-frequency, long-range coupling between prefrontal and visual cortex during attention. *Science, 324*, 1207–1210.

Grube, M., & Griffiths, T. D. (2009). Metrically-enhanced temporal coding and the subjective perception of rhythmic sequences. *Cortex, 45*, 72–79.

Hartmann, T., Schlee, W., & Weisz, N. (2012). It's only in your head: Expectancy of aversive auditory stimulation modulates stimulus-induced auditory cortical alpha desynchronization. *Neuroimage, 60*, 170–178.

Henry, M. J., & Hermann, B. (2014). Low-frequency neural oscillations support dynamic attending in temporal context. *Timing Time Percept.*, *2*, 62–86.

Huron, D. (2006). *Sweet anticipation: Music and the psychology of expectation*. Cambridge, MA, USA: The MIT Press.

Iversen, J. R., Repp, B. H., & Patel, A. D. (2009). Top-down control of rhythm perception modulates early auditory responses. *Ann. N.Y. Acad. Sci., 1169*, 58–73.

Jensen, O., Bonnefond, M., & VanRullen, R. (2012). An oscillatory mechanism for prioritizing salient unattended stimuli. *Trends Cogn. Sci., 15*, 200–206.

Jones, M. R. (1976). Time, our lost dimension: Toward a new theory of perception, attention, and memory. *Psychol. Rev.*, *83*, 323–355.

Jones, M. R., & Boltz, M. (1989). Dynamic attending and responses to time. *Psychol. Rev.*, *96*, 459–491.

Klimesch, W., Sauseng, P., & Hanslmayr, S. (2007). EEG alpha oscillations: The inhibition-timing hypothesis. *Brain Res. Rev.*, *53*, 63–88.

Krishnan, A., Williams, L. J., McIntosh, A. R., & Abdi, H. (2011). Partial Least Squares (PLS) methods for neuroimaging: A tutorial and review. *Neuroimage*, *56*, 455–475.

Lakatos, P., Karmos, G., Mehta, A. D., Ulbert, I., & Schroeder, C. E. (2008). Entrainment of neuronal oscillations as a mechanism of attentional selection. *Science, 320*, 110–113.

Large, E. W. (2008). Resonating to musical rhythm: theory and experiment. In S. Grondin (Ed.). *The psychology of time* (pp. 189–232). West Yorkshire, UK: Emerald.

Large, E. W., & Jones, M. R. (1999). The dynamics of attending: How we track time-varying events. *Psychol. Rev., 106*, 119–159.

Large, E. W., & Snyder, J. S. (2009). Pulse and meter as neural resonance. *Ann. N.Y. Acad. Sci., 1169*, 46–57.

Lerdahl, F., & Jackendoff, R. (1983). *A generative theory of tonal music.* Cambridge, MA, USA: The MIT Press.

Levitt, H. (1971). Transformed up-down methods in psychoacoustics. *J. Acoust. Soc. Am., 49*, 467–477.

McIntosh, A. R., & Lobaugh, N. J. (2004). Partial least squares analysis of neuroimaging data:

Applications and advances. *Neuroimage*, *23*, S250–263.

Melloni, L., Schwiedrzik, C. M., Rodriguez, E., & Singer, W. (2009). (Micro)Saccades, corollary activity and cortical oscillations. *Trends Cogn. Sci., 13*, 239–245.

Nozaradan, S., Peretz, I., Missal, M., & Mouraux, A. (2011). Tagging the neuronal entrainment to beat and meter. *J. Neurosci., 31*, 10234–10240.

Nozaradan, S., Peretz, I., & Mouraux, A. (2012). Selective entrainment to beat and meter embedded in a musical rhythm. *J. Neurosci., 32*, 17572–17581.

Palmer, C., & Krumhansl, C. L. (1990). Mental representations of musical meter. *J. Exp. Psychol. Hum. Percept Perform., 16*, 728–741.

Potter, D. D., Fenwick, M., Abecasis, D., & Brochard, R. (2009). Perceiving rhythm where none exists: Event-related potential (ERP) correlates of subjective accenting. *Cortex, 45*,103–109.

Repp, B. H. (2005). Sensorimotor synchronization: A review of the tapping literature. *Psychol. Bull. Rev.*, *12*, 969–992.

Repp, B. H., & Su, Y.-H. (2013). Sensorimotor synchronization: A review of recent research (2006–2012). *Psychol. Bull. Rev., 20*, 403–452.

Rodgers, J. L. (1999). The bootstrap, the jackknife, and the randomization test: A sampling taxonomy. *Multivariate Behav. Res.*, *34*, 441–456.

Ronken, D. (1970). Monaural detection of a phase difference between clicks. *J. Acoust. Soc. Am., 47*, 1091–1099.

Rothermich, K., Schmidt-Kassow, M., & Kotz, S. A. (2012). Rhythm's gonna get you: Regular meter facilitates semantic sentence processing. *Neuropsychologia, 50*, 232–244.

Scavone, G. (2001). RtAudio: A set of realtime audio i/o C++ classes [computer software]. McGill University, Montreal, QC, Canada.

Schaefer, R. S., Vlek, R. J., & Desain, P. (2011). Decomposing rhythm processing: Electroencephalography of perceived and self-imposed rhythmic patterns. *Psychol. Res. 75*, 95–106.

Schroeder, C. E., & Lakatos, P. (2009). Low-frequency neuronal oscillations as instruments of sensory selection. *Trends Neurosci., 32*, 9–18.

Snyder, J. S., & Large, E. W. (2005). Gamma-band activity reflects the metric structure of rhythmic tone sequences. *Cogn. Brain Res., 24*,117–126.

Soley, G., & Hannon, E. E. (2010). Infants prefer the musical meter of their own culture: A cross-cultural comparison. *Dev. Psychol., 46*, 286–292.

Tissen, M. A., Marsden, J. F., & Brown, P. (2000). Frequency analysis of EMG activity in patients with idiopathic torticollis. *Brain, 123*, 677–686.

Van Boxtel, A. (2001). Optimal signal bandwidth for the recording of surface EMG activity of facial, jaw, oral, and neck muscles. *Psychophysiology, 38*, 22–34.

van Noorden, L., & Moelants, D. (1999). Resonance in the perception of musical pulse. *J. New Music Res., 28*, 43–66.

Ward, L. (2003). Synchronous neural oscillations and cognitive processes. *Trends Cogn. Neurosci.*, *7*, 553–559.

Weisz, N, Hartmann, T., Müller, N., Lorenz, I., & Obleser, J. (2011). Alpha rhythms in audition: Cognitive and clinical perspectives. *Front. Psychol. 2*, 73. doi:10.3389/fpsyg.2011.00073.